



Elasticity solutions of functionally graded piezoelectric plates under electric fields in cylindrical bending

Shixue Liang, Yuanxie Shen, Fangyuan Cai, Lulu Shen and Bo Yang

Abstract. This paper presents elasticity solutions for functionally graded piezoelectric plates under electric fields in cylindrical bending. Based on the generalized Mian and Spencer plate theory, the assumption of the material parameters which can vary along the thickness direction of the plate in an arbitrary fashion is kept; however, the materials are extended from elastic materials to piezoelectric materials. The electric potential function is constructed following the forms of the displacement functions in Mian and Spencer plate theory. The essential idea of Mian and Spencer plate theory (J Mech Phys Solids 46:2283–2295, 1998) is that the three-dimensional elasticity equations for inhomogeneous materials can be obtained by two-dimensional solution for homogeneous materials by straightforward substitutions. Through rigorous derivation, the corresponding elasticity solutions of cylindrical bending of functionally graded piezoelectric plates under electric fields are obtained. In the numerical examples, the accuracy of the present solutions is verified and the responses of plates subjected to electrical potential difference and electrical displacement are investigated, respectively.

Mathematics Subject Classification. 74B20, 74F20, 74K20.

Keywords. Functionally graded piezoelectric plate, Electric field, Cylindrical bending, Mian and Spencer plate theory, Elasticity solution.

1. Introduction

Piezoelectric materials have been considered as promising candidates for actuators and sensors applied in micro-electro-mechanical and smart systems due to their intrinsic coupling of the electric field and the electric field [1]. Traditional piezoelectric devices are designed as laminated forms of piezoelectric materials, which easily cause interfacial debonding and high-stress concentrations under mechanical or electric loadings. Inspired by the concept of functionally graded materials, functionally graded piezoelectric materials (FGPMs) have been developed, whose composition and properties can be designed smoothly and continuously in the preferred orientation [1, 2].

Currently, numerical, semi-analytic and analytic methods have been proposed to investigate the mechanical/piezoelectric responses of FGPM plates [3–19]. Semi-analytical methods, combined analytical methods with numerical methods, have been developed for the static, free vibration and buckling analyses of FGPM plates with various boundary conditions [4–6]. For example, semi-analytical solutions were elaborated based on the extended Stroh-like formalism for 3D static problems of electro-elastic mono- and multilayered plates, where mechanical and electrical forces were applied on the top and/or bottom layer and may take arbitrary forms [5]; Wu and Ding [6] employed a unified formulation of the finite layer method, based on the Reissner mixed variational theorem, for the coupled electro-elastic analysis of the simply-supported FGPM plates under electro-mechanical loads. As for numerical methods, such as the differential quadrature (DQ), finite element (FE) and meshless methods, which have been adopted for more complex problems of FGPM plates [8–10]. For instants, geometrically nonlinear static response

of functionally graded piezoelectric plate under mechanical and electrical loads was studied by using Meshless method [9]. Radial point interpolation method (RPIM) was used to create the shape function and approximate the field variables. The first-order shear deformation plate theory (FSDT) and Von Karman strains were used to model the nonlinear behavior of plate; Kumar and Harsha [10] executed a modal analysis of functionally graded piezoelectric material rectangular plate to find the natural frequency with different mode shapes by using the FE Technique where the piezoelectric material was considered to be graded along the thickness according to the simplified power-law.

Although the analytical methods are limited to the relatively simple problems, the availability of analytical solutions with the highest accuracy is inherently of much importance to serve as a benchmark for numerical and semi-analytical modeling [11]. Based on the three-dimensional (3D) piezoelectricity theory and the state space approach, Zhong and Shang [12] obtained an exact solution of a simply-supported FGPM rectangular plate with exponent-law distribution under the sinusoidal mechanical and electric loadings. Li et al. [13, 14] and Zhao et al. [15] adopted the direct displacement method to perform a 3D analysis of the transversely isotropic FGPM circular plates subjected to a uniform mechanical loading, electric potential difference and electric displacement on the upper and/or lower surfaces, respectively. Li and Pan [16] investigated the static bending problems of a simply supported FGPM microplate with considering the size effect, and the material properties were varied through the thickness according to a power law. Liu and Wang [17] obtained 3D analytical solutions for the structural instability of a simply supported orthotropic piezoelectric rectangular microplate by means of a linear perturbation analysis. An analytical solution was presented by Ghafarollahi and Shodja [18] for the scattering of transverse surface waves by a homogeneous piezoelectric fiber contained in a functionally graded piezoelectric half-space with exponentially varying electromechanical properties using a multipole expansion method. Zenkour and Hafed [19] presented the piezoelectric effect on the bending of simply supported FGPM plate by using a simple quasi-3D sinusoidal shear deformation theory, in which material properties were assumed to vary exponentially in the thickness direction. Besides, Bachir et al. [20, 21] developed a refined shear deformation theory with four unknown functions to obtain the elastic solutions of the thermo-mechanical bending response for the functionally graded plate. As the reviewed papers mentioned above, it is worth noting that due to the mathematical difficulties, not much work has been done to obtain elasticity solutions of FGPM plates based on piezoelectricity theory.

Mian and Spencer [22] developed an ingenious theory for deriving 3D analytical solutions for isotropic FGM plates with tractions-free surfaces. In this theory, the material properties are assumed to vary arbitrarily in the thickness direction of plates. The origins of this method can be traced back to the classical solutions by Michell [23] for plane stress of moderately thick elastic plates. Yang et al. [24, 25] extended above Mian and Spencer plate theory to study transversely isotropic FGM plates subjected to uniform loads applied on the top and bottom surfaces. In this paper, we further extend the generalized Mian and Spencer plate theory for deriving elasticity solutions of the equations of linear piezoelectricity for FG piezoelectric materials, which are no longer the elastic materials and reveal the innovation of the present work. This is not a trivial extension because the elastic deformation and electric field are coupled for piezoelectric materials. To illustrate the procedure of this extension, functionally graded piezoelectric plates under electric fields in cylindrical bending are investigated and the corresponding elasticity solutions are presented. The proposed theory will be helpful for the further investigation on related boundary value problems of FGPM plates.

2. Basic equations

In a rectangular Cartesian coordinate (x, y, z) , consider an orthotropic and FGPM plate of uniform thickness h , shown in Fig. 1a, with the xy plane at mid-plane ($z = 0$) and z -axis perpendicular to the mid-plane. It is noteworthy that the material parameters are varied arbitrarily along the z -axis. As shown

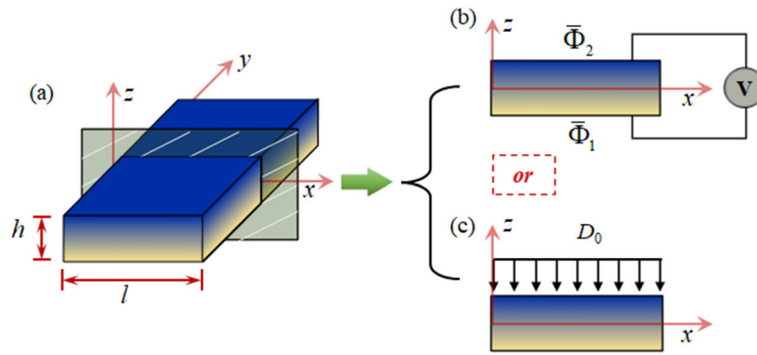


FIG. 1. **a** 3D FGPM plate and coordinate system; 2D FGPM plates subjected to an **(b)** electric potential difference and **c** electric displacement

in Figs. 1b, c, two typical external electric loadings are applied, respectively, that is, a uniform electric potential difference ($\bar{\Phi}_2$ at $z = h/2$ and $\bar{\Phi}_1$ at $z = -h/2$) and electric displacement D_0 are uniformly distributed on the top and/or bottom surfaces the of plate. When the plate is in a state of cylindrical bending, the geometrical dimension of the plate along the y -axis is assumed to be far longer than the other two directions such that $0 \leq x \leq l$ $-\infty < y < \infty$ and $-h/2 \leq z \leq h/2$ and then, the three-dimensional (3D) plate problem can be simplified to a two-dimensional (2D) plane problem where all.

In the absence of body forces, the basic equations for piezoelectricity are given in the following [24]:

$$\sigma_{x,x} + \tau_{xz,z} = 0, \quad \tau_{xz,x} + \sigma_{z,z} = 0. \quad (1)$$

$$D_{x,x} + D_{z,z} = 0, \quad (2)$$

$$\sigma_x = c_{11}u_{,x} + c_{13}w_{,z} + e_{31}\phi_{,z}, \quad \sigma_z = c_{13}u_{,x} + c_{33}w_{,z} + e_{33}\phi_{,z}, \quad \tau_{zx} = c_{55}(u_{,z} + w_{,x}) + e_{15}\phi_{,x}, \quad (3)$$

$$D_x = e_{15}(u_{,z} + w_{,x}) - \lambda_{11}\phi_{,x}, \quad D_z = e_{31}u_{,x} + e_{33}w_{,z} - \lambda_{33}\phi_{,z} \quad (4)$$

where the comma denotes differentiation with respect to the indicated variable; σ_x , σ_z and τ_{xz} are the stress components; u and w are the displacement components; D_x and D_z are the electric displacements; ϕ is the electric potential; c_{ij} , e_{ij} and λ_{ij} are the elastic, piezo-electric and dielectric coefficients, respectively. It is noteworthy that these elastic coefficients are functions of z for FGPMs, and particularly become constant coefficients for homogeneous materials.

Based on the generalized Mian and Spencer plate theory [22], we seek solutions of the displacements as follows:

$$\begin{aligned} u(x, z) &= \bar{u}(x) + F(z)\bar{u}_{,xx} + A(z)\bar{w}_{,x} + B(z)\bar{w}_{,xxx}, \\ w(x, z) &= \bar{w}(x) + G(z)\bar{u}_{,x} + C(z)\bar{w}_{,xx} + D(z), \end{aligned} \quad (5)$$

where $A(z)$, $B(z)$, $C(z)$, $D(z)$, $F(z)$, $G(z)$ are the unknown functions to be determined Assume functions $\bar{u} = \bar{u}(x)$ and $\bar{w} = \bar{w}(x)$ are the mid-plane displacements of the plate and hence, we have $A(0) = 0$, $B(0) = 0$, $C(0) = 0$, $D(0) = 0$, $F(0) = 0$, $G(0) = 0$ from Eq. (5).

Following the above expression forms of the displacements, it is assumed that the electric potential function has the following form:

$$\phi(x, z) = \phi_1(z)\bar{u}_{,x} + \phi_2(z)\bar{w}_{,xx} + \phi_0(z), \quad (6)$$

where $\phi_0(z)$, $\phi_1(z)$, $\phi_2(z)$ are the unknown functions to be determined

Substituting Eqs. (5)–(6) into Eqs. (3)–(4), the expressions of the stress components and electric displacement components are rewritten as:

$$\sigma_x = \bar{u}_{,x}(c_{11} + c_{13}G' + e_{31}\phi_1') + \bar{w}_{,xx}(c_{11}A + c_{13}C' + e_{31}\phi_2') + Fc_{11}\bar{u}_{,xxx} + Bc_{11}\bar{w}_{,xxxx}$$

$$\begin{aligned}
& +D'c_{13}+e_{31}\phi'_0, \\
\sigma_z & = \bar{u}_{,x}(c_{13}+c_{33}G'+e_{33}\phi'_1)+\bar{w}_{,xx}(c_{13}A+c_{33}C'+e_{33}\phi'_2)+Fc_{13}\bar{u}_{,xxx}+Bc_{13}\bar{w}_{,xxxx} \\
& +D'c_{33}+e_{33}\phi'_0, \\
\tau_{zx} & = \bar{u}_{,xx}[c_{55}(F'+G)+e_{15}\phi_1]+\bar{w}_{,xxx}[c_{55}(B'+C)+e_{15}\phi_2]+\bar{w}_{,x}[c_{55}(A'+1)], \tag{7}
\end{aligned}$$

$$\begin{aligned}
D_x & = \bar{u}_{,xx}[e_{15}(F'+G)-\lambda_{11}\phi_1]+\bar{w}_{,xxx}[e_{15}(B'+C)-\lambda_{11}\phi_2]+\bar{w}_{,x}[e_{15}(A'+1)], \\
D_z & = \bar{u}_{,x}(e_{31}+e_{33}G'-\lambda_{33}\phi'_1)+\bar{w}_{,xx}(e_{31}A+e_{33}C'-\lambda_{33}\phi'_2)+e_{31}F\bar{u}_{,xxx}+e_{31}B\bar{w}_{,xxxx} \\
& +e_{33}D'-\lambda_{33}\phi'_0. \tag{8}
\end{aligned}$$

Substituting Eqs. (7)–(8) into Eqs. (1)–(2) and provided that:

$$[c_{55}(A'+1)]' = 0, \tag{9}$$

$$(c_{13}+c_{33}G'+e_{33}\phi'_1)' = 0, \tag{10}$$

$$(e_{31}+e_{33}G'-\varepsilon_{33}\phi'_1)' = 0, \tag{11}$$

$$c_{55}(A'+1)+(c_{13}A+c_{33}C'+e_{33}\phi'_2)' = 0, \tag{12}$$

$$e_{15}(A'+1)+(e_{31}A+e_{33}C'-\varepsilon_{33}\phi'_2)' = 0, \tag{13}$$

$$c_{11}+c_{13}G'+e_{31}\phi'_1+(c_{55}(F'+G)+e_{15}\phi_1)' = c_{55}\kappa_1, \tag{14}$$

$$c_{11}A+c_{13}C'+e_{31}\phi'_2+(c_{55}(B'+C)+e_{15}\phi_2)' = c_{55}\kappa_2, \tag{15}$$

$$\bar{u}_{,xxx} = \kappa_3, \tag{16}$$

$$\bar{w}_{,xxxx} = \kappa_4. \tag{17}$$

where “ $'$ ” denotes differentiation with respect to z , and κ_i ($i = 1, 2, 3, 4$) are arbitrary constant to be determined.

Accordingly, Eqs. (1)–(2) are rewritten as:

$$\kappa_1\kappa_3 + \kappa_2\kappa_4 = 0. \tag{18}$$

$$[c_{55}(F'+G)+(Fc_{13})'+e_{15}\phi_1]\kappa_3+[c_{55}(B'+C)+(c_{13}B)'+e_{15}\phi_2]\kappa_4+(c_{33}D'+e_{33}\phi'_0)' = 0, \tag{19}$$

$$[e_{15}(F'+G)+(Fe_{31})'-\varepsilon_{11}\phi_1]\kappa_3+[e_{15}(B'+C)+(e_{31}B)'-\varepsilon_{11}\phi_2]\kappa_4+(e_{33}D'-\varepsilon_{33}\phi'_0)' = 0. \tag{20}$$

The mid-plane displacement components can be given by integrating Eqs. (16)–(17), respectively:

$$\bar{w}(x) = \frac{1}{24}\kappa_4x^4 + \frac{1}{6}C_1x^3 + \frac{1}{2}C_2x^2 + C_3x + C_4, \tag{21}$$

$$\bar{u}(x) = \frac{1}{6}\kappa_3x^3 - \frac{1}{2}\frac{\kappa_2}{\kappa_1}C_1x^2 + C_5x + C_6. \tag{22}$$

where C_i ($i = 1, 2, \dots, 6$) are integral constants to be determined by the edge boundary conditions at $x = 0, l$

3. Under electric potential case

3.1. Determination of the displacement functions and electric potential functions

When only electric potential is applied, the boundary conditions on the top and bottom surfaces of the plate can be expressed as:

$$z = -h/2: \quad \sigma_z = 0, \quad \tau_{zx} = 0, \quad \phi = \bar{\Phi}_1 \tag{23}$$

$$z = h/2: \quad \sigma_z = 0, \quad \tau_{zx} = 0, \quad \phi = \bar{\Phi}_2 \tag{24}$$

The expression of the electric potential function in Eq. (6) is updated by introducing Eqs. (21)–(22):

$$\phi(x, z) = \frac{\kappa_3 \phi_1(z) + \kappa_4 \phi_2(z)}{2} x^2 - \left[\frac{\kappa_2}{\kappa_1} \phi_1(z) - \phi_2(z) \right] C_1 x + \phi_1(z) C_5 + \phi_2(z) C_2 + \phi_0(z). \quad (25)$$

Substituting Eq. (7) and Eq. (25) into Eqs. (23)–(24) leads to the following differential equations:

$$A'(\pm h/2) + 1 = 0, \quad (26)$$

$$c_{13}(\pm h/2) + c_{33}(\pm h/2) G'(\pm h/2) + e_{33}(\pm h/2) \phi_1'(\pm h/2) = 0, \quad (27)$$

$$c_{13}(\pm h/2) A(\pm h/2) + c_{33}(\pm h/2) C'(\pm h/2) + e_{33}(\pm h/2) \phi_2'(\pm h/2) = 0, \quad (28)$$

$$c_{13}(\pm h/2) [\kappa_3 F(\pm h/2) + \kappa_4 B(\pm h/2)] + c_{33}(\pm h/2) D'(\pm h/2) + e_{33}(\pm h/2) \phi_0'(\pm h/2) = 0 \quad (29)$$

$$c_{55}(\pm h/2) [F'(\pm h/2) + G(\pm h/2)] + e_{15}(\pm h/2) \phi_1(\pm h/2) = 0 \quad (30)$$

$$c_{55}(\pm h/2) [B'(\pm h/2) + C(\pm h/2)] + e_{15}(\pm h/2) \phi_2(\pm h/2) = 0 \quad (31)$$

$$\kappa_3 \phi_1(\pm h/2) + \kappa_4 \phi_2(\pm h/2) = 0 \quad (32)$$

$$\phi_1(-h/2) C_5 + \phi_2(-h/2) C_2 + \phi_0(-h/2) = \bar{\Phi}_1 \quad (33)$$

$$\phi_1(h/2) C_5 + \phi_2(h/2) C_2 + \phi_0(h/2) = \bar{\Phi}_2 \quad (34)$$

Integrating Eqs. (9)–(15) and (19)–(20) by virtue of Eqs. (26)–(34), the expressions of functions of variable z in Eqs. (5) and (6) can be determined:

$$A(z) = -z \quad (35)$$

$$B(z) = k_2 f_5(z) - \Phi_2 f_6(z) + H_4 f_7(z) + B_1(z) + B_0, \quad (36)$$

$$C(z) = C_1(z) + H_4 a_0^0(z) + C_0, \quad (37)$$

$$D(z) = -\kappa_3 [D_{00}(z) H_2 + D_{01}(z)] - \kappa_4 [D_{00}(z) H_4 + D_{02}(z)] + a_0^0(z) H_7 + D_0 \quad (38)$$

$$F(z) = k_1 f_5(z) - \Phi_1 f_6(z) + H_2 f_7(z) + F_1(z) + F_0, \quad (39)$$

$$G(z) = G_1(z) + H_2 a_0^0(z) + G_0, \quad (40)$$

$$\phi_1(z) = \phi_{10}(z) - H_2 b_0^0(z) + \Phi_1 \quad (41)$$

$$\phi_2(z) = \phi_{20}(z) - H_4 b_0^0(z) + \Phi_2, \quad (42)$$

$$\phi_0(z) = -\kappa_3 [\phi_{00}(z) H_2 + \phi_{01}(z)] - \kappa_4 [\phi_{00}(z) H_4 + \phi_{02}(z)] - b_0^0(z) H_7 + \Phi_0, \quad (43)$$

where the expressions of functions including $a_0^0(z)$, $b_0^0(z)$, $F_1(z)$, $B_1(z)$, $f_i(z)$ ($i = 5, 6, 7$), $D_{0i}(z)$ ($i = 0, 1, 2$), $\phi_{0i}(z)$ ($i = 0, 1, 2$) are listed in ‘‘Appendix A’’; B_0 , C_0 , D_0 , F_0 , G_0 , Φ_1 , Φ_2 , Φ_0 , H_2 , H_4 and H_7 are integration constants, in which H_2 , H_4 and H_7 can be expressed according to Eqs. (8), (10) and (11):

$$H_2 = e_{31} + e_{33} G'(z) - \lambda_{33} \phi_1'(z), \quad H_4 = e_{31} A + e_{33} C'(z) - \lambda_{33} \phi_2'(z),$$

$$H_7 = \kappa_3 e_{31} (-h/2) F(-h/2) + \kappa_4 e_{31} (-h/2) B(-h/2) + e_{33} (-h/2) D'(-h/2) - \lambda_{33} (-h/2) \phi_0'(-h/2)$$

3.2. Determination of the remaining integral constants

Integrating Eqs. (14)–(15) gives:

$$\kappa_1 = \frac{\int_{-h/2}^{h/2} c_{11} + c_{13} G' + e_{31} \phi_1' d\xi}{\int_{-h/2}^{h/2} c_{55} d\xi} = \frac{h_0^0(h/2) - H_2 f_0^0(h/2)}{g_5(h/2)},$$

$$\kappa_2 = \frac{\int_{-h/2}^{h/2} c_{11}A + c_{13}C' + e_{31}\phi_2' d\xi}{\int_{-h/2}^{h/2} c_{55}d\xi} = \frac{-h_1^0(h/2) - H_4 f_0^0(h/2)}{g_5(h/2)} \tag{44}$$

where $g_5(z) = \int_{-h/2}^z c_{55}d\xi$, and $h_i^j(z)$ ($i, j = 0, 1$) is given in ‘‘Appendix A’’.

Substituting Eqs. (41)–(42) into Eq. (32) leads to:

$$\kappa_3\Phi_1 + \kappa_4\Phi_2 = 0, \tag{45}$$

$$\kappa_3 [\phi_{10}(h/2) - H_2 b_0^0(h/2)] + \kappa_4 [\phi_{20}(h/2) - H_4 b_0^0(h/2)] = 0. \tag{46}$$

Integrating Eq. (19) and using Eq. (29) with $z = h/2$, we can obtain the following expression:

$$\kappa_3 \int_{-h/2}^{h/2} [c_{55}(F' + G) + e_{15}\phi_1]d\xi + \kappa_4 \int_{-h/2}^{h/2} [c_{55}(B' + C) + e_{15}\phi_2]d\xi = 0. \tag{47}$$

Substituting Eqs. (36)–(43) into above Eq. (47) leads to

$$\kappa_3 [-h_0^1(h/2) + H_2 f_0^1(h/2)] + \kappa_4 [h_1^1(h/2) + H_4 f_0^1(h/2)] = 0. \tag{48}$$

Substituting Eq. (44) into (18), Eqs. (46)–(48) become:

$$\begin{aligned} & [f_1^0(h/2) f_0^0(h/2) - b_0^0(h/2) h_1^0(h/2)] H_2 + [f_0^0(h/2) f_0^0(h/2) - b_0^0(h/2) h_0^0(h/2)] H_4 \\ & = f_1^0(h/2) h_0^0(h/2) - f_0^0(h/2) h_1^0(h/2), \end{aligned} \tag{49}$$

$$\begin{aligned} & [h_1^1(h/2) f_0^0(h/2) - f_0^1(h/2) h_1^0(h/2)] H_2 + [h_0^1(h/2) f_0^0(h/2) - f_0^1(h/2) h_0^0(h/2)] H_4 \\ & = h_1^1(h/2) h_0^0(h/2) - h_0^1(h/2). \end{aligned} \tag{50}$$

Thus, constants H_2 and H_4 can be determined by solving these two simultaneous equations.

Furthermore, we define the mean values of electric displacement along x -axis at $x = 0, l$ as [13–15]

$$D_x^* = \frac{1}{h} \int_{-h/2}^{h/2} D_x dz = 0. \tag{51}$$

We can arrive at the following expressions from Eq. (51):

$$\begin{aligned} \Phi_1 &= \frac{1}{h/2} \int_{-h/2}^{h/2} \{e_{15}[F'(z) + G(z)] - \lambda_{11}[\phi_{10}(z) - H_2 b_0^0(z)]\} d\xi, \\ \Phi_2 &= \frac{1}{h/2} \int_{-h/2}^{h/2} \{e_{15}[B'(z) + C(z)] - \lambda_{11}[\phi_{20}(z) - H_4 b_0^0(z)]\} d\xi \end{aligned} \tag{52}$$

By considering the fact that $\phi(0, 0) = \phi(l, 0)$ for the FGPM plate in this case, we obtain the following equation:

$$\frac{1}{2} [\kappa_3 \phi_1(0) + \kappa_4 \phi_2(0)] l^2 - C_1 \left[\frac{\kappa_2}{\kappa_1} \phi_1(0) - \phi_2(0) \right] l = 0. \tag{53}$$

Accordingly, we can obtain the expressions of κ_3 and κ_4 by using Eqs. (18) and (53):

$$\kappa_3 = \frac{2}{l} \frac{\kappa_2}{\kappa_1} C_1, \quad \kappa_4 = -\frac{2}{l} C_1. \quad (54)$$

Introducing Eqs. (41)–(43) into Eqs. (33)–(34), we have the following equation:

$$\begin{aligned} & \frac{2}{l} \left\{ \frac{\kappa_2}{\kappa_1} [\phi_{01}(h/2)] - \phi_{02}(h/2) \right\} C_1 - [f_1^0(h/2) + H_4 b_0^0(h/2)] C_2 \\ & + [f_0^0(h/2) - H_2 b_0^0(h/2)] C_5 - b_{00}(h/2) H_7 = \bar{\Phi}_2 - \bar{\Phi}_1. \end{aligned} \quad (55)$$

The six integral constants C_i ($i = 1, 2, \dots, 6$) arising from Eq. (21)–(22) can be determined by the edge boundary conditions at $x = 0, l$, which there are simply supported (**S**), clamped (**C**) and free (**F**) conditions:

$$\mathbf{S} : \quad \bar{u} = 0, \quad \bar{w} = 0, \quad M_x = 0, \quad (56)$$

$$\mathbf{C} : \quad \bar{u} = 0, \quad \bar{w} = 0, \quad \bar{w}_{,x} = 0, \quad (57)$$

$$\mathbf{F} : \quad N_x = 0, \quad M_x = 0, \quad Q_x = 0, \quad (58)$$

where the expressions of the resultant forces and moments are given in ‘‘Appendix B’’. There are totally 4 different kinds of combination of Eqs. (56)–(58), namely SS, CC, SC, CF, in which the first letter denotes the conditions at $x = 0$ and the second signifies those at $x = l$. For any kind of the above-mentioned boundary conditions, we have six equations from boundary conditions and a supplementary equation from Eq. (55) which are just enough to determine constants: C_i ($i = 1, 2, \dots, 6$) and H_7 completely.

Therefore, the elasticity solutions of FGPM plates under the external electric potentials can be obtained from Eqs. (3)–(5).

4. Under electric displacement case

4.1. Determination of the displacement and electric potential functions

When an electric displacement is applied on the top surface of the plate, the boundary conditions on the top and bottom surfaces are proposed as

$$z = -h/2 : \quad \sigma_z = 0, \quad \tau_{zx} = 0, \quad D_z = 0 \quad (59)$$

$$z = h/2 : \quad \sigma_z = 0, \quad \tau_{zx} = 0, \quad D_z = -D_0 \quad (60)$$

Similarly, substituting the related stress and electric displacement components in Eqs. (7)–(8) into Eqs. (59)–(60), and in view of Eqs. (26)–(31), the following equations can be gotten:

$$e_{31}(\pm h/2) + e_{33}(\pm h/2) G'(\pm h/2) - \lambda_{33}(\pm h/2) \phi'_1(\pm h/2) = 0, \quad (61)$$

$$e_{31}(\pm h/2) A(\pm h/2) + e_{33}(\pm h/2) C'(\pm h/2) - \lambda_{33}(\pm h/2) \phi'_2(\pm h/2) = 0, \quad (62)$$

$$\begin{aligned} & e_{31}(-h/2) F(-h/2) \kappa_3 + e_{31}(-h/2) B(-h/2) \kappa_4 + e_{33}(-h/2) D'(-h/2) \\ & - \lambda_{33}(-h/2) \phi'_0(-h/2) = 0, \end{aligned} \quad (63)$$

$$\begin{aligned} & e_{31}(+h/2) F(+h/2) \kappa_3 + e_{31}(+h/2) B(+h/2) \kappa_4 + e_{33}(+h/2) D'(+h/2) \\ & - \lambda_{33}(+h/2) \phi'_0(+h/2) = -D_0. \end{aligned} \quad (64)$$

Based on some of Eqs. (9)–(15), and Eqs. (19)–(20), (26)–(31) and (61)–(64), the displacement and electric potential functions can be easily deduced:

$$A(z) = -z \quad (65)$$

$$B(z) = \int_{-h/2}^z \frac{1}{c_{55}} [B_{10}(\xi) - e_{15}\phi_2(\xi)] - C(\xi)d\xi + B_0, \quad (66)$$

$$C(z) = - \int_{-h/2}^z \frac{\lambda_{33}c_{13} + e_{33}e_{31}}{c_{33}\lambda_{33} + e_{33}^2} A(\xi)d\xi + C_0, \quad (67)$$

$$D(z) = - \int_{-h/2}^z \frac{\lambda_{33} [D_{10}(\xi) + D_{00}(\xi)] + e_{33} [D_{20}(\xi) + D_{01}(\xi)]}{c_{33}\lambda_{33} + e_{33}^2} d\xi + D_0, \quad (68)$$

$$F(z) = \int_{-h/2}^z \frac{1}{c_{55}} [F_{10}(\xi) - e_{15}\phi_1(\xi)] - G(\xi)d\xi + F_0, \quad (69)$$

$$G(z) = - \int_{-h/2}^z \frac{\lambda_{33}c_{13} + e_{33}e_{31}}{c_{33}\lambda_{33} + e_{33}^2} d\xi + G_0, \quad (70)$$

$$\phi_1(z) = \int_{-h/2}^z \frac{c_{33}e_{31} - c_{13}e_{33}}{c_{33}\lambda_{33} + e_{33}^2} d\xi + \Phi_1, \quad (71)$$

$$\phi_2(z) = \int_{-h/2}^z \frac{c_{33}e_{31} - c_{13}e_{33}}{c_{33}\lambda_{33} + e_{33}^2} A(\xi) d\xi + \Phi_2, \quad (72)$$

$$\phi_0(z) = \int_{-h/2}^z \frac{c_{33} [D_{20}(\xi) + D_{01}(\xi)] - e_{33} [D_{10}(\xi) + D_{00}(\xi)]}{c_{33}\lambda_{33} + e_{33}^2} d\xi + \Phi_0, \quad (73)$$

where the expressions of functions $F_{10}(z)$, $B_{10}(z)$, $D_{10}(z)$, $D_{00}(z)$, $D_{20}(z)$ and $D_{01}(z)$ are listed in ‘‘Appendix C’’; B_0 , C_0 , D_0 , F_0 , G_0 , Φ_1 , Φ_2 and Φ_0 are integration constants which revealed in ‘‘Appendix C’’.

4.2. Determination of the remaining integral constants

The determination of κ_1 and κ_2 is similar to the electric potential case with integrating Eqs. (10)–(11), while κ_3 and κ_4 can be obtained via the following equations which can be obtained by integrating Eqs. (19)–(20) with the aid of Eqs. (63)–(64):

$$\kappa_3 \int_{-h/2}^{h/2} [c_{55} (F' + G) + e_{15}\phi_1]d\xi + \kappa_4 \int_{-h/2}^{h/2} [c_{55} (B' + C) + e_{15}\phi_2]d\xi = 0 \quad (74)$$

$$\kappa_3 \int_{-h/2}^{h/2} [e_{15} (F' + G) - \lambda_{11}\phi_1]d\xi + \kappa_4 \int_{-h/2}^{h/2} [e_{15} (B' + C) - \lambda_{11}\phi_2]d\xi = D_0 \quad (75)$$

Considering the boundary conditions at $x = 0, l$ (as shown in Eqs. (56)–(58)), six integral constants, $C_i (i = 1, 2, \dots, 6)$ can be determined by six equations provided by any two kind of boundary conditions. Accordingly, the elasticity solutions of FGPM plate under the external electric displacement can be obtained completely from Eqs. (3)–(5).

TABLE 1. Constants of some typical piezoelectric materials

Property	PZT-4 [14]	BATIO ₃ [27]	COFE ₂ O ₄ [27]
Elastic (10 ⁹ N/m ²)	$c_{11}^0=139.0, c_{33}^0=115.0,$	$c_{11}^B=166.0, c_{33}^B=162.0,$	$c_{11}^C=286.0, c_{33}^0=269.5,$
Piezoelectric (C/m ²)	$c_{13}^0=74.3, c_{55}^0=25.6$ $e_{31}^0=-5.2, e_{33}^0=15.1,$	$c_{13}^C=78.0, c_{55}^C=43.0$ $e_{31}^C=-4.4, e_{33}^C=18.6,$	$c_{13}^C=170.5, c_{55}^C=45.3$ $e_{31}^B=0, e_{33}^B=0, e_{15}^B=0$
Dielectric (10 ⁻⁹ C/(Vm))	$e_{15}^0=12.7$ $\lambda_{11}^0=6.5, \lambda_{33}^0=5.6$	$e_{15}^C=11.6$ $\lambda_{11}^C=11.2, \lambda_{33}^0=12.6$	$\lambda_{11}^C=0.08, \lambda_{33}^0=0.093$

TABLE 2. Comparison of \bar{W} and $\bar{\sigma}_x$ at top and bottom surfaces

z/h	CC				SS			
	\bar{W}		$\bar{\sigma}_x$		\bar{W}		$\bar{\sigma}_x$	
	-0.5	0.5	-0.5	0.5	-0.5	0.5	-0.5	0.5
Present	4.3746	-4.3790	-7.1766	-7.1766	5.4683	-5.4738	-5.0954	-5.0954
FEM	4.5293	-4.5293	-6.9947	-6.9947	5.5638	-5.5638	-5.0090	-5.0090
Errors (%)	-3.42	-3.32	2.60	2.60	-1.72	-1.62	1.72	1.72

5. Numerical results and discussion

To illustrate the present elasticity solutions, numerical examples are given in this section to reveal the electrical responses of FGPM plates subjected to a uniform electric potential difference and electric displacement, respectively. Unless stated otherwise, the thickness of FGPM plate $h = 0.15$ m, the width $l = 1$ m, and $x = l/2$ in this work. Note that the material parameters can be varied arbitrarily along the thickness direction in this paper

5.1. Verification

The verification of the proposed analytical solutions is performed via a homogeneous piezoelectric plate subjected to a uniform electric potential difference. We compare the present results with a numerical model which are established by ABAQUS software via finite element method (FEM). The 8-node reduced integration element (C3D8R) is adopted to mesh the plate, and the material property of piezoelectric material PZT-4 is listed in Table 1. An incremental electric potential difference (1V) is applied between the top and bottom surfaces of the plate to obtain the piezoelectric responses.

Taking CC and SS boundary conditions as typical examples to prove the accuracy of the present analytical solutions for brevity. Figure 2 shows the distributions of the dimensionless deflection \bar{W} ($\bar{W} = W/h$) and normal stress component $\bar{\sigma}_x$ ($\bar{\sigma}_x = \sigma_x/c_{11}^0$) along the thickness direction of the plate. It is obviously that the present solutions are in excellent agreement with FEM results. As shown in Table 2, the absolute errors of the dimensionless deflection \bar{W} and normal stress $\bar{\sigma}_x$ are less than 3.42% and 2.60%, respectively. These results indicate that the present analytical solution is valid and accuracy in predicting the piezoelectric responses of plates.

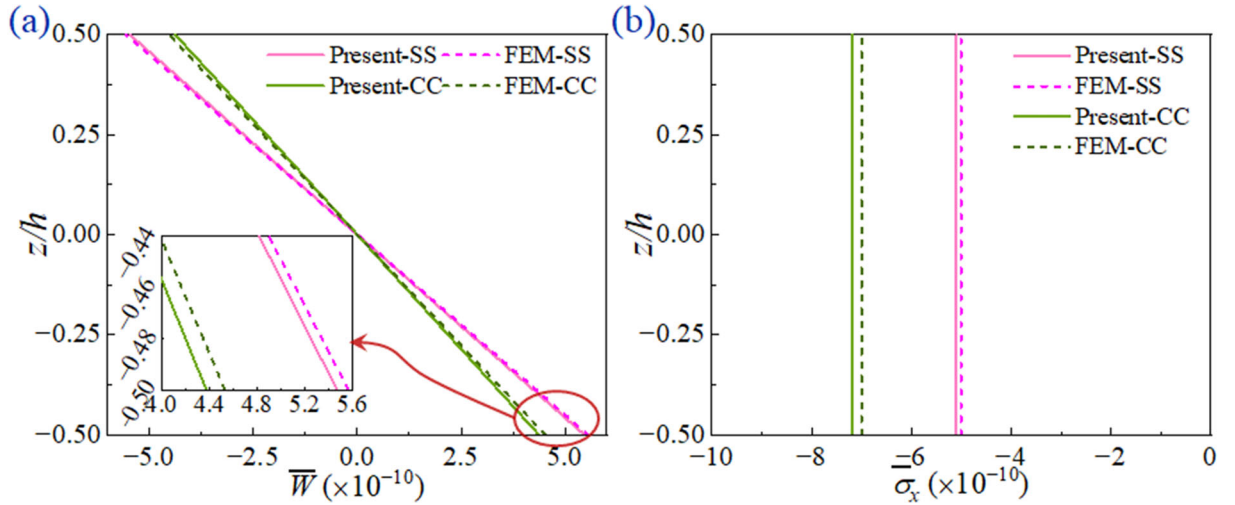


FIG. 2. Comparison of dimensionless **a** deflection \bar{W} and **b** stress component $\bar{\sigma}_x$ between the present and FEM results

5.2. Under electric potential case

We now consider a FGPM plate subjected to a uniform electric potential difference with $\bar{\Phi}_1 = 0$ and $\bar{\Phi}_2 = 1V$ and with material properties varied exponentially along the z -direction [18]:

$$c_{ij}(z) = c_{ij}^0 e^{[(z+h/2)/h]p}, \quad e_{ij}(z) = e_{ij}^0 e^{[(z+h/2)/h]p}, \quad \lambda_{ij}(z) = \lambda_{ij}^0 e^{[(z+h/2)/h]p}, \quad i, j = 1, 2, \dots, 6, \quad (76)$$

where p is the gradient index to characterize the degree of material inhomogeneity. In Particular, the FGPM will degrade into the homogenous piezoelectric material if $p = 0$. c_{ij}^0 , e_{ij}^0 and λ_{ij}^0 are the elastic, piezoelectric and dielectric properties of PZT-4 [14] (given in Table 1) at the bottom surface ($z = -h/2$) of plate, respectively. Without loss of generality, CS boundary condition is considered in this case. Moreover, the following dimensionless quantities are introduced:

$$\bar{W} = \frac{W}{h}, \quad \bar{\sigma}_x = \frac{\sigma_x}{c_{11}^0}, \quad \bar{\Phi}^* = \frac{\phi}{(\bar{\Phi}_2 - \bar{\Phi}_1)}, \quad \bar{D}_z = \frac{D_z}{\sqrt{c_{11}^0 \epsilon_{33}^0}}. \quad (77)$$

Figure 3a plots the variations of the dimensionless electric potential $\bar{\Phi}^*$ with the p changed from -10 to 10 along the thickness direction of the plate. It is found that $\bar{\Phi}^*$ changes in a linear way when $p = 0$. As for the FGPMs, $\bar{\Phi}^*$ exhibits an obvious nonlinear behavior. Affected by the distribution characteristics of exponential function in Eq. (76), $\bar{\Phi}^*$ firstly increases sharply and then, shows a slowly increase when $p > 0$, while $\bar{\Phi}^*$ firstly show a relatively gentle rising and then, increases significantly when $p < 0$. Moreover, these trends are becoming apparent with the increased absolute value of p . The dimensionless electric displacement component \bar{D}_z for various values of p along the thickness direction of plate is shown in Fig. 3b. It is observed that the distributions of \bar{D}_z basically keep constant along the thickness direction of the plate, and the absolute value is increasing with p changed from -10 to 10.

When it comes to the elastic field, the through-the-thickness distributions of the dimensionless deflection \bar{W} are presented in Fig. 4a. It is easy to observe that \bar{W} tends to zero at the mid-plane of plate regardless of p . \bar{W} shows a linear trend for homogeneous materials and has an evident nonlinear change for FGPMs. When $p > 0$, the maximum deflection occurs on the bottom surface of the FGPM plate; when $p < 0$, the maximum value of the absolute deflection achieved on the top surface. It is also obvious that \bar{W} is central symmetric for the same absolute value of p . Figure 4b displays the variation of dimensionless normal stress $\bar{\sigma}_x$ along the thickness direction of plate. The distribution pattern of $\bar{\sigma}_x$ is the same as that

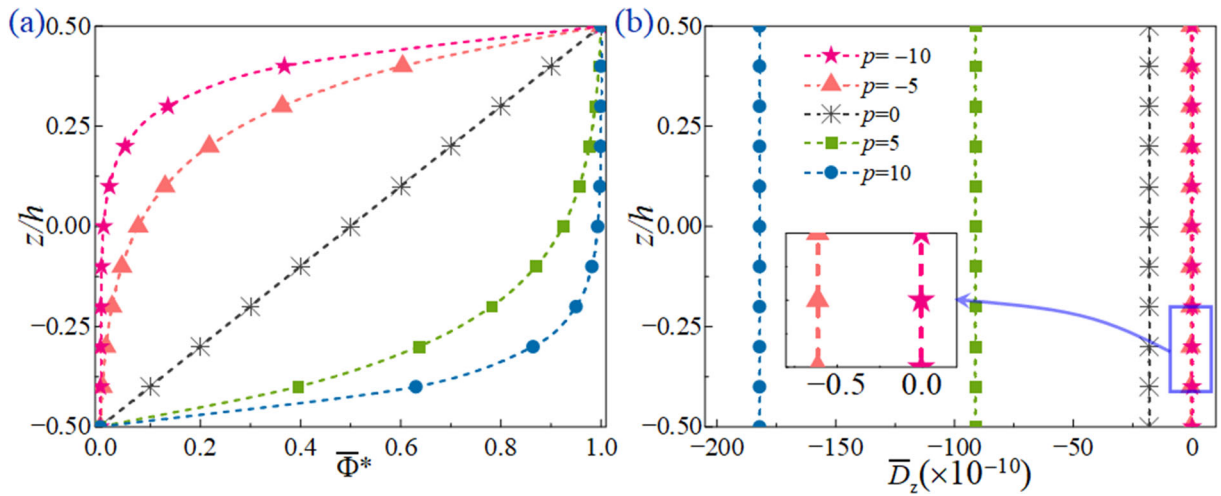


FIG. 3. Distribution of dimensionless **a** electric potential $\bar{\Phi}^*$ and **b** electric displacement component \bar{D}_z along the thickness direction of plate

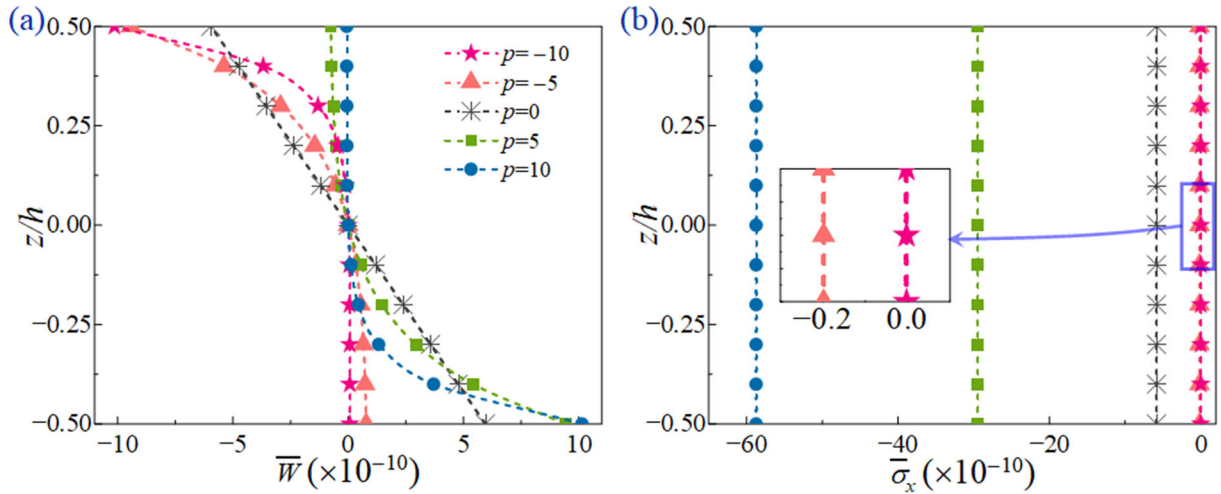


FIG. 4. Dimensionless **a** deflection \bar{W} and **b** stress component $\bar{\sigma}_x$ along the thickness direction of plate

of \bar{D}_z , which means that $\bar{\sigma}_x$ keeps constant along the thickness direction of plate and the absolute value increases with p .

5.3. Under electric displacement case

Next, we consider a FGPM plate subjected to an external electric displacement $D_0=0.01C/m^2$ uniformly distributed on the top surface of plate. The material properties vary in a power law manner [15]:

$$c_{ij}(z) = c_{ij}^B (1/2 - z/h)^p + c_{ij}^C [1 - (1/2 - z/h)^p],$$

$$e_{ij}(z) = e_{ij}^B (1/2 - z/h)^p + e_{ij}^C [1 - (1/2 - z/h)^p],$$

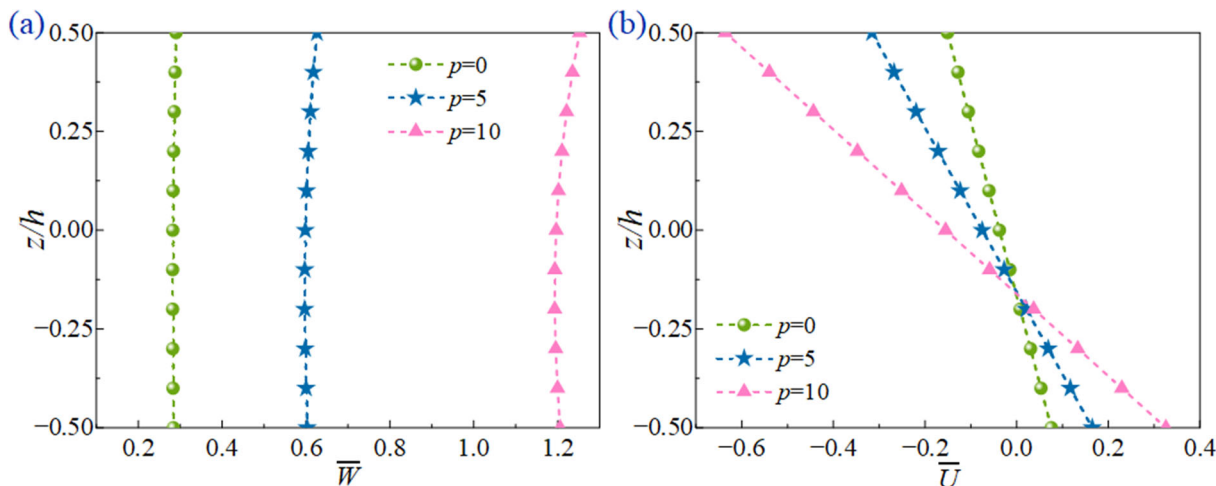


FIG. 5. Dimensionless displacements a \bar{W} and b \bar{U} along the thickness direction of plate

$$\lambda_{ij}(z) = \lambda_{ij}^B (1/2 - z/h)^p + \lambda_{ij}^C [1 - (1/2 - z/h)^p], \quad i, j = 1, 2, \dots, 6, \quad (78)$$

where c_{ij}^B , e_{ij}^B , λ_{ij}^B , c_{ij}^C , e_{ij}^C and λ_{ij}^C are material coefficients of BaTiO₃ and CoFe₂O₄(listed in Table 1) [27]. The gradient index $p = 0$ corresponds to BaTiO₃ material. We take a FGPM plate with CF boundary condition as a typical example in this case, and a set of dimensionless variables are introduced for the sake of display:

$$\bar{U} = \frac{u}{h}, \quad \bar{W} = \frac{W}{h}, \quad \bar{\sigma}_x = \frac{\sigma_x}{c_{11}^C}, \quad \bar{\sigma}_z = \frac{\sigma_z}{c_{11}^C}, \quad \bar{\Phi}^* = \frac{\phi}{h} \sqrt{\frac{\lambda_{33}^C}{c_{33}^C}}, \quad \bar{D}_z = \frac{D_z}{D_0}. \quad (79)$$

Figure 5 shows the variations of the dimensionless displacements \bar{W} and \bar{U} along the thickness direction of the plate. The material gradient index p is taken for 0, 5 and 10. In contrast to the case of the homogeneous piezoelectric material ($p = 0$) where \bar{W} appears linear distribution along thickness direction in Fig. 5a, it becomes increasingly nonlinear distribution with increased p . Besides, it can be found that the value of \bar{W} increases with p . The dimensionless in-plane displacement \bar{U} shows a linear variation across the thickness direction in Fig. 5b. The maximal absolute value of \bar{U} occurs at the top surface of the plate, which also increases with p .

Distributions of the dimensionless stresses $\bar{\sigma}_x$ and $\bar{\sigma}_z$ along the thickness direction of the plate are illustrated in Fig. 6. It can be observed that $\bar{\sigma}_x$ basically presents a linear distribution through the thickness direction, while $\bar{\sigma}_z$ exhibit obvious nonlinear change characteristics. The maximal absolute values of $\bar{\sigma}_x$ and $\bar{\sigma}_z$ are gained on the top surface and in the upper half of the plates, respectively. We can see that $\bar{\sigma}_z$ on the top and bottom surfaces of plate exactly meet the boundary conditions in Eqs. (59)–(60). Moreover, compared with $\bar{\sigma}_x$, $\bar{\sigma}_z$ is a high-order small quantity which is consistent with that under mechanical loading.

As illustrated in Fig. 7a, the dimensionless electric displacement \bar{D}_z is nonlinear along the thickness direction for FGPMs as compared with a linear distribution for the homogeneous piezoelectric material ($p = 0$). Moreover, the curve of the dimensionless electric potential $\bar{\Phi}^*$ is plotted in Fig. 7b which shows a nonlinear change along the thickness direction of the plate.

Furthermore, the effects of the boundary conditions, including SS, CC, CS and CF, on the thickness distributions of \bar{W} , $\bar{\sigma}_x$ and $\bar{\Phi}^*$ are revealed in Figs. 8a–c with $p = 10$. As shown in Fig. 8a, \bar{W} has negative values for the SS, CC and CS cases and obtains positive value for the CF case. Besides, \bar{W} gains the

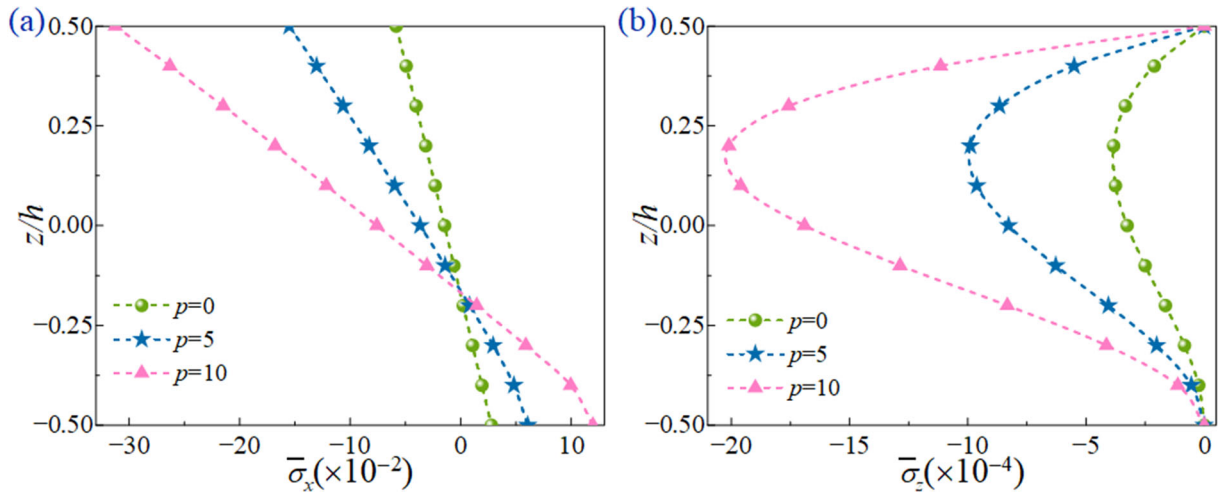


FIG. 6. Dimensionless stress component **a** $\bar{\sigma}_x$ and **b** $\bar{\sigma}_z$ along the thickness direction of plate

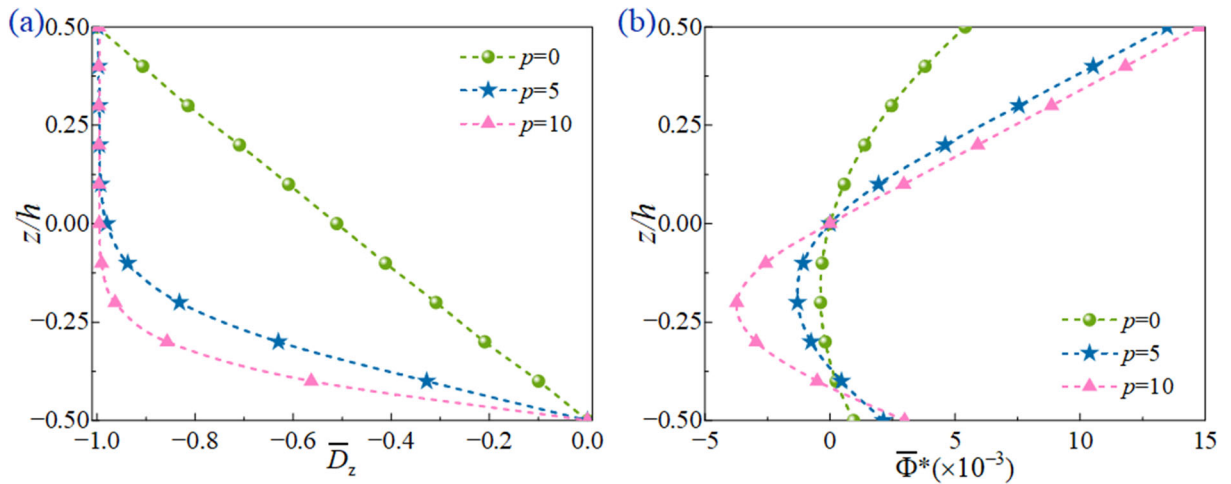


FIG. 7. Dimensionless **a** electric displacement component \bar{D}_z and **b** electric potential $\bar{\Phi}^*$ along the thickness direction of plate

maximal absolute value for the SS boundary condition. As for $\bar{\sigma}_x$ in Fig. 8b, the maximal absolute values appear on the top surface of the FGPM plates in which the CF plate has the maximum value. As shown in Fig. 8c, it is obvious that the distributions of $\bar{\Phi}^*$ exhibit mainly no difference for all boundary conditions within the upper part of the FGPM plates, while there is a significant difference in the lower part of the plates.

6. Conclusions

Elasticity solutions of FGPM plates under electric fields in cylindrical bending are presented in this paper. The main conclusions are as follows:

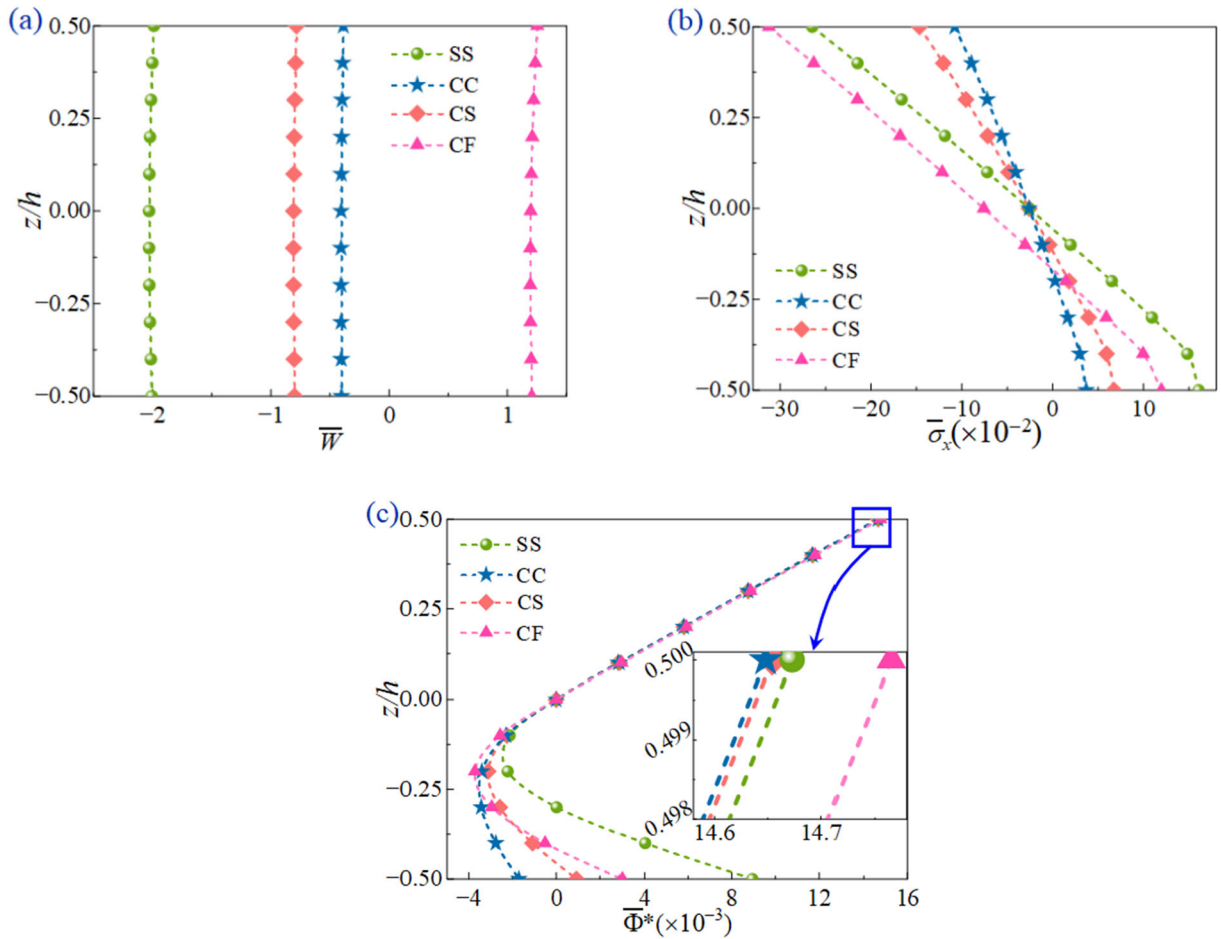


FIG. 8. Dimensionless **a** displacement \bar{W} , **b** stress component $\bar{\sigma}_x$ and **c** electric potential $\bar{\Phi}^*$ along the thickness direction of plate with $p = 10$

1. The generalized Mian and Spencer plate theory is extended by constructing the electric potential functions referring to the forms of the displacement components, such that the boundary conditions on the top and bottom surfaces of plate are exactly satisfied;
2. The present analytical solutions are verified through comparison with the FEM results with the aid of ABAQUS software, which shows an excellent agreement;
3. In the numerical examples, a uniformly distributed electrical potential difference and electrical displacement are applied on the top and bottom surfaces of plate, respectively. It is concluded that the gradient index of material p , the edge boundary conditions and the distribution model of material properties have a remarkable influence on the elastic and electric fields in the FGPM plates;
4. Since the present theory can deal with FGPM plates with arbitrary distribution model of material properties and arbitrary edge boundary conditions, it indicates that the electro-mechanical responses of FGPM plates under electric fields can be actively controlled and optimized by regulating above-mentioned influencing factors.

It should also be emphasized that the present theory is within the framework of piezoelectricity. The proposed piezoelectricity solutions can serve as good benchmarks for the study of problem in the paper based on various simplified plate theories or numerical methods.

Acknowledgements

This work is supported by the National Natural Science Foundation of China (Nos. 11872336, 51808499), Project of State Key Laboratory for Strength and Vibration of Mechanical Structures (Nos. SV2020-KF-13) and the Science Foundation of Zhejiang Province of China (No. LY22E080016, LQ21A020009).

Author contributions S.L. and L.S. wrote the main manuscript text; Y.S. and F.C prepared the figures and tables; Y.S. performed the numerical simulation; B.Y. reviewed and edited the manuscript. All authors reviewed the manuscript.

Declarations

Conflict of interest The authors declare no competing interests.

Publisher's Note Springer Nature remains neutral with regard to jurisdictional claims in published maps and institutional affiliations.

Springer Nature or its licensor (e.g. a society or other partner) holds exclusive rights to this article under a publishing agreement with the author(s) or other rightsholder(s); author self-archiving of the accepted manuscript version of this article is solely governed by the terms of such publishing agreement and applicable law.

Appendix A: Expressions of the introduced functions related to variable z and integral constants in electric potential case

$$g_i^n(z) = \int_{-h/2}^z (z - \xi)^n \xi^i \frac{\lambda_{33}c_{13} + e_{33}e_{31}}{c_{33}\lambda_{33} + e_{33}^2} d\xi, \quad (i, n = 0, 1)$$

$$h_i^n(z) = \int_{-h/2}^z (z - \xi)^n \xi^i \left(c_{11} - c_{13} \frac{c_{13}\lambda_{33} + e_{33}e_{31}}{c_{33}\lambda_{33} + e_{33}^2} - e_{31} \frac{c_{13}e_{33} - c_{33}e_{31}}{e_{33}^2 + c_{33}\lambda_{33}} \right) d\xi, \quad (i, n = 0, 1),$$

$$f_i^n(z) = \int_{-h/2}^z (z - \xi)^n \xi^i \frac{c_{33}e_{31} - c_{13}e_{33}}{c_{33}\lambda_{33} + e_{33}^2} d\xi, \quad (i, n = 0, 1),$$

$$a_i^n(z) = \int_{-h/2}^z (z - \xi)^n \xi^i \frac{e_{33}}{c_{33}\lambda_{33} + e_{33}^2} d\xi, \quad (i, n = 0, 1),$$

$$b_i^n(z) = \int_{-h/2}^z (z - \xi)^n \xi^i \frac{c_{33}}{c_{33}\lambda_{33} + e_{33}^2} d\xi, \quad (i, n = 0, 1),$$

$$f_5(z) = \int_{-h/2}^z \frac{g_5(\xi)}{c_{55}} d\xi, \quad f_6(z) = \int_{-h/2}^z \frac{e_{15}}{c_{55}} d\xi,$$

$$\begin{aligned}
f_7(z) &= \int_{-h/2}^z \left\{ \frac{f_0^0(\xi) + e_{15}b_0^0(\xi)}{c_{55}} - [a_0^0(\xi) - a_0^0(0)] \right\} d\xi, \\
f_{16}(z) &= \int_{-h/2}^z \left\{ \frac{e_{15}}{c_{55}} [f_0^0(\xi) + e_{15}b_0^0(\xi)] + b_0^0(\xi) \lambda_{11} \right\} d\xi, \\
f_{17}(z) &= \int_{-h/2}^z \left\{ \frac{e_{15}}{c_{55}} [h_0^0(\xi) + e_{15}f_0^0(\xi)] + f_0^0(\xi) \lambda_{11} \right\} d\xi, \\
f_{18}(z) &= \int_{-h/2}^z \left\{ \frac{e_{15}}{c_{55}} [h_1^0(\xi) + e_{15}f_1^0(\xi)] + f_1^0(\xi) \lambda_{11} \right\} d\xi, \\
k_{31}^*(z) &= c_{13} [F_1(z) + F_0] - h_0^1(z), \quad k_{32}^*(z) = e_{31} [F_1(z) + F_0] - f_{17}(z), \\
k_{33}^*(z) &= c_{13} f_7(z) + f_0^1(z), \quad k_{41}^*(z) = c_{13} [B_1(z) + B_0] + h_1^1(z), \\
k_{42}^*(z) &= e_{31} [B_1(z) + B_0] + f_{18}(z), \quad k_{44}^*(z) = e_{31} f_7(z) + f_{16}(z), \\
B_1(z) &= - \int_{-h/2}^z \left\{ \frac{1}{c_{55}} [h_1^0(\xi) + e_{15}f_1^0(\xi)] - [g_1^0(z) - g_1^0(0)] \right\} d\xi, \\
C_1(z) &= g_1^0(z) \quad D_{00}(z) = \int_{-h/2}^z \left[\frac{k_{33}^*(\xi) \lambda_{33} + k_{44}^*(\xi) e_{33}}{c_{33} \lambda_{33} + e_{33}^2} \right] d\xi, \\
D_{01}(z) &= \int_{-h/2}^z \left[\frac{k_{31}^*(\xi) \lambda_{33} + k_{32}^*(\xi) e_{33}}{c_{33} \lambda_{33} + e_{33}^2} \right] d\xi, \quad D_{02}(z) = \int_{-h/2}^z \left[\frac{k_{41}^*(\xi) \lambda_{33} + k_{42}^*(\xi) e_{33}}{c_{33} \lambda_{33} + e_{33}^2} \right] d\xi, \\
F_1(z) &= - \int_{-h/2}^z \left\{ \frac{1}{c_{55}} [h_0^0(\xi) + e_{15}f_0^0(\xi)] - [g_0^0(\xi) - g_0^0(0)] \right\} d\xi, \\
G_1(z) &= -g_0^0(z), \quad \phi_{10}(z) = f_0^0(z), \quad \phi_{20}(z) = -f_1^0(z), \\
\phi_{00}(z) &= \int_{-h/2}^z \left[\frac{k_{33}^*(\xi) e_{33} - k_{44}^*(\xi) c_{33}}{c_{33} \lambda_{33} + e_{33}^2} \right] d\xi, \\
\phi_{01}(z) &= \int_{-h/2}^z \left[\frac{k_{31}^*(\xi) e_{33} - k_{32}^*(\xi) c_{33}}{c_{33} \lambda_{33} + e_{33}^2} \right] d\xi, \\
\phi_{02}(z) &= \int_{-h/2}^z \left[\frac{k_{41}^*(\xi) e_{33} - k_{42}^*(\xi) c_{33}}{c_{33} \lambda_{33} + e_{33}^2} \right] d\xi,
\end{aligned}
\tag{A-1}$$

$$\begin{aligned}
B_0 &= -k_2 f_5(0) + \Phi_2 f_6(0) - H_4 f_7(0) - B_1(0), \\
C_0 &= -g_1^0(0) - H_4 a_0^0(0), \\
D_0 &= \kappa_3 [D_{00}(z) H_2 + D_{01}(z)] + \kappa_4 [D_{00}(z) H_4 + D_{02}(z)] - a_0^0(z) H_7, \\
F_0 &= -k_1 f_5(0) + \Phi_1 f_6(0) - H_2 f_7(0) - F_1(0),
\end{aligned}$$

$$G_0 = g_0^0(0) - H_2 a_0^0(0), \quad \Phi_0 = \bar{\Phi}_1 - (\Phi_2 C_2 + \Phi_1 C_5). \quad (\text{A-2})$$

Appendix B: Expressions of stress resultants and moments

$$\begin{aligned} N_x &= \int_{-h/2}^{h/2} \sigma_x dz = N_1 \bar{u}_{,x} + N_3 \bar{w}_{,xx} + N_5 \bar{u}_{,xxx} + N_7 \bar{w}_{,xxxx} + N_0 \\ M_x &= \int_{-h/2}^{h/2} \sigma_x z dz = M_1 \bar{u}_{,x} + M_3 \bar{w}_{,xx} + M_5 \bar{u}_{,xxx} + M_7 \bar{w}_{,xxxx} + M_0 \\ Q_x &= \int_{-h/2}^{h/2} \tau_{zx} dz = Q_1 \bar{u}_{,xx} + Q_2 \bar{w}_{,xxx} \end{aligned} \quad (\text{B-1})$$

where

$$\begin{aligned} N_1 &= \int_{-h/2}^{h/2} (c_{11} + c_{13}G' + e_{31}\phi'_1) dz, \quad N_3 = \int_{-h/2}^{h/2} (c_{11}A + c_{13}C' + e_{31}\phi'_2) dz, \\ N_5 &= \int_{-h/2}^{h/2} c_{11}F dz, \quad N_7 = \int_{-h/2}^{h/2} c_{11}B dz, \quad N_0 = \int_{-h/2}^{h/2} c_{13}D' + e_{31}\phi'_0 dz, \\ M_1 &= \int_{-h/2}^{h/2} z (c_{11} + c_{13}G' + e_{31}\phi'_1) dz, \quad M_3 = \int_{-h/2}^{h/2} z (c_{11}A + c_{13}C' + e_{31}\phi'_2) dz, \\ M_5 &= \int_{-h/2}^{h/2} c_{11}zF dz, \quad M_7 = \int_{-h/2}^{h/2} c_{11}zB dz, \quad M_0 = \int_{-h/2}^{h/2} (c_{13}D' + e_{31}\phi') z dz, \\ Q_1 &= \int_{-h/2}^{h/2} [c_{55}(F' + G) + e_{15}\phi_1] dz, \quad Q_2 = \int_{-h/2}^{h/2} [c_{55}(B' + C) + e_{15}\phi_2] dz, \end{aligned} \quad (\text{B-2})$$

Appendix C: Expressions of the introduced functions related to variable z and integral constants in electric displacement case

$$\begin{aligned} F_{10}(z) &= \int_{-h/2}^z [c_{55}\kappa_1 - c_{11} - c_{13}G'(\xi) - e_{31}\phi'_1(\xi)] d\xi, \\ B_{10}(z) &= \int_{-h/2}^z [c_{55}\kappa_2 - c_{11}A(\xi) - c_{13}C'(\xi) - e_{31}\phi'_2(\xi)] d\xi, \\ D_{00} &= c_{13}(-h/2) [\kappa_3 F(-h/2) + \kappa_4 B(-h/2)], \end{aligned}$$

$$\begin{aligned}
D_{01} &= e_{31}(-h/2) [\kappa_3 F(-h/2) + \kappa_4 B(-h/2)], \\
D_{10}(z) &= \int_{-h/2}^z \left\{ \kappa_3 [c_{55}(F' + G) + (Fc_{13})' + e_{15}\phi_1] + \kappa_4 [c_{55}(B' + C) + (c_{13}B)' + e_{15}\phi_2] \right\} d\xi, \\
D_{20}(z) &= \int_{-h/2}^z \left\{ \kappa_3 [e_{15}(F' + G) + (Fe_{31})' - \lambda_{11}\phi_1] + \kappa_4 [e_{15}(B' + C) + (e_{31}B)' - \lambda_{11}\phi_2] \right\} d\xi, \quad (\text{C-1}) \\
B_0 &= - \int_{-h/2}^0 \left\{ \frac{1}{c_{55}} [B_{10}(z) - e_{15}\phi_2(z)] - C(z) \right\} dz, \\
C_0 &= \int_{-h/2}^0 \left[\frac{\lambda_{33}c_{13} + e_{33}e_{31}}{c_{33}\lambda_{33} + e_{33}^2} A(z) \right] dz, \\
D_0 &= \int_{-h/2}^0 \left\{ \frac{\lambda_{33} [D_{10}(z) + D_{00}(z)] + e_{33} [D_{20}(z) + D_{01}(z)]}{c_{33}\lambda_{33} + e_{33}^2} \right\} dz, \\
F_0 &= - \int_{-h/2}^0 \left\{ \frac{1}{c_{55}} [F_{10}(z) - e_{15}\phi_1] - G(z) \right\} dz, \quad G_0 = \int_{-h/2}^0 \left(\frac{\lambda_{33}c_{13} + e_{33}e_{31}}{c_{33}\lambda_{33} + e_{33}^2} \right) dz, \\
\Phi_1 &= - \int_{-h/2}^0 \left(\frac{c_{33}e_{31} - c_{13}e_{33}}{c_{33}\lambda_{33} + e_{33}^2} \right) dz, \quad \Phi_2 = - \int_{-h/2}^0 \left[\frac{c_{33}e_{31} - c_{13}e_{33}}{c_{33}\lambda_{33} + e_{33}^2} A(z) \right] dz, \\
\Phi_0 &= - \int_{-h/2}^0 \left\{ \frac{c_{33} [D_{20}(z) + D_{01}(z)] - e_{33} [D_{10}(z) + D_{00}(z)]}{c_{33}\lambda_{33} + e_{33}^2} \right\} dz. \quad (\text{C-2})
\end{aligned}$$

References

- [1] Wu, C.C.M., Kahn, M., Moy, W.: Piezoelectric ceramics with functional gradients: a new application in material design. *J. Am. Ceram. Soc.* **79**, 809–812 (1996)
- [2] Zhu, X., Meng, Z.: Operational principle, fabrication and displacement characteristics of a functionally gradient piezoelectric ceramic actuator. *Sens. Actuat. A-Phys.* **48**(3), 169–176 (1995)
- [3] Zhang, S., Zhao, G., Rao, M.N., Schmidt, R., Yu, Y.: A review on modeling techniques of piezoelectric integrated plates and shells. *J. Intel. Mat. Syst. Str.* **30**(8), 1133–1147 (2019)
- [4] Wu, C., Liu, Y.: A review of semi-analytical numerical methods for laminated composite and multilayered functionally graded elastic/piezoelectric plates and shells. *Compos. Struct.* **147**, 1–15 (2016)
- [5] Magouh, N., Azrar, L., Alnefaie, K.: Semi-analytical solutions of static and dynamic degenerate, nondegenerate and functionally graded electro-elastic multilayered plates. *Appl. Math. Model.* **114**, 722–744 (2023)
- [6] Wu, C., Ding, S.: Coupled electro-elastic analysis of functionally graded piezoelectric material plates. *Smart. Struct. Syst.* **16**(5), 781–806 (2015)
- [7] Nguyen, N.V., Lee, J.: On the static and dynamic responses of smart piezoelectric functionally graded graphene platelet-reinforced microplates. *Int. J. Mech. Sci.* **197**, 106310 (2021)
- [8] Zhong, Z., Wu, L., Chen, W.: Progress in the study on mechanics problems of functionally graded materials and structures. *Adv. Mech.* **40**(5), 528–541 (2010)
- [9] Nourmohammadi, H., Behjat, B.: Geometrically nonlinear analysis of functionally graded piezoelectric plate using mesh-free RPIM. *Eng. Anal. Bound. Elem.* **99**, 131–141 (2019)

- [10] Kumar, P., Harsha, S.P.: Modal analysis of functionally graded piezoelectric material plates. *Mater. Today Proc.* **28**, 1481–1486 (2020)
- [11] Muradova, A.D., Stavroulakis, G.E.: Mathematical models with buckling and contact phenomena for elastic plates: a review. *Mathematics* **8**(4), 566 (2020)
- [12] Zhong, Z., Shang, E.T.: Three-dimensional exact analysis of a simply supported functionally gradient piezoelectric plate. *Int. J. Solids. Struct.* **40**(20), 5335–5352 (2003)
- [13] Li, X., Ding, H., Chen, W.: Three-dimensional analytical solution for a transversely isotropic functionally graded piezoelectric circular plate subject to a uniform electric potential difference. *Sci. China. Ser. G.* **51**(8), 1116–1125 (2008)
- [14] Li, X., Wu, J., Ding, H., Chen, W.: 3D analytical solution for a functionally graded transversely isotropic piezoelectric circular plate under tension and bending. *Int. J. Eng. Sci.* **49**(7), 664–676 (2011)
- [15] Zhao, X., Li, X., Li, Y.: Axisymmetric analytical solutions for a heterogeneous multi-Ferroic circular plate subjected to electric loading. *Mech. Adv. Mater. Struct.* **25**(10), 795–804 (2017)
- [16] Li, Y., Pan, E.: Static bending and free vibration of a functionally graded piezoelectric microplate based on the modified couple-stress theory. *Int. J. Eng. Sci.* **97**, 40–59 (2015)
- [17] Liu, L., Wang, X.: Three-dimensional analytical solution for the instability of a parallel array of mutually attracting identical simply supported piezoelectric microplates. *Z. Angew. Math. Phys.* **68**(6), 136 (2017)
- [18] Ghafarollahi, A., Shodja, H.M.: Scattering of transverse surface waves by a piezoelectric fiber in a piezoelectric half-space with exponentially varying electromechanical properties. *Z. Angew. Math. Phys.* **70**(2), 66 (2019)
- [19] Zenkour, A.M., Hafez, Z.S.: Bending analysis of functionally graded piezoelectric plates via quasi-3D trigonometric theory. *Mech. Adv. Mater. Struct.* **27**(18), 1551–1562 (2019)
- [20] Boudierba, B., Berrabah, H.M.: Bending response of porous advanced composite plates under thermomechanical loads. *Mech. Based Des. Struct.* **50**(9), 3262–3282 (2020)
- [21] Boudierba, B., Hamza Madjid, B., Pham, D.T.: Bending analysis of P-FGM plates resting on nonuniform elastic foundations and subjected to thermo-mechanical loading. *Cogent Eng.* **9**(1), 2108576 (2022)
- [22] Mian, M.A., Spencer, A.J.M.: Exact solutions for functionally graded and laminated elastic materials. *J. Mech. Phys. Solids.* **46**(12), 2283–2295 (1998)
- [23] Michell, J.H.: On the direct determination of stress in an elastic solid, with application to the theory of plates. *Proc. Lond. Math. Soc.* **31**(1), 100–124 (1899)
- [24] Yang, B., Ding, H., Chen, W.: Elasticity solutions for functionally graded plates in cylindrical bending. *Appl. Math. Mech.* **29**(8), 999–1004 (2008)
- [25] Yang, B., Ding, H., Chen, W.: Elasticity solutions for a uniformly loaded rectangular plate of functionally graded materials with two opposite edges simply supported. *Acta Mech.* **207**(3), 245–258 (2009)
- [26] Ding, H., Chen, W.: *Three Dimensional Problems of Piezoelectricity*. Nava Science Publishers, New York (2001)
- [27] Wu, C., Tsai, Y.: Static behavior of functionally graded magneto-electro-elastic shells under electric displacement and magnetic flux. *Int. J. Eng. Sci.* **45**(9), 744–769 (2007)

Shixue Liang, Yuanxie Shen, Fangyuan Cai, Lulu Shen and Bo Yang
School of Civil Engineering and Architecture
Zhejiang Sci-Tech University
Hangzhou 310018
China
e-mail: yangbo@zstu.edu.cn

(Received: February 9, 2023; revised: May 16, 2023; accepted: May 23, 2023)